DEVELOPING AND EVALUATING A HYBRID WIND INSTRUMENT EXCITED BY A LOUDSPEAKER

K Buys The Open University, Milton Keynes, Buckinghamshire, UK
D Sharp The Open University, Milton Keynes, Buckinghamshire, UK
R Laney The Open University, Milton Keynes, Buckinghamshire, UK

1 INTRODUCTION

The concept of hybrid wind instrumentation is explained in figure 1: a physical model of a mouthpiece (including the player's mouth) is simulated on a real-time computer and interacts with a real acoustical resonator so that the whole is able to generate self-sustained sounds.

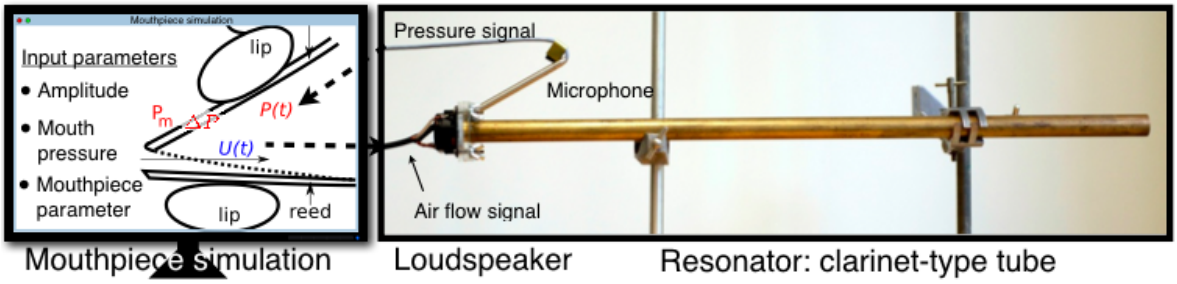

Figure 1: The hybrid wind instrument set-up: a computed mouthpiece in interaction with a physical resonator by means of a loudspeaker.

Such a device has two main research uses. First, placing it in the context of acoustic wind instrument research, it would be of substantial value to have a repeatable and precisely quantified control over an exciter that is linked to a resonator of interest. This matches with the objectives of the now classical "artificial mouths" for wind instruments[1,2]. The opposite concept is also of interest: studying how the excitation relates to the produced sound, by comparison with real and simulated wind instruments and wind instrument theories[3].
A second interest is the exploration of the device's potential as a musical instrument, lying mostly in the timbre domain, which is an active musical composition focus of today[4,5]. Here, the same control precision can play a role in the accessibility of certain (variations of) sounds. While, the computed environment allows modelling any conceivable excitation and handles electronic parameter variations, the physical control over the resonator (the fingering) remains, which opens up an alternative range of musical expression with the advantage of relatively low computational power needs.
Only minor contributions on this topic have been made to date. Maganza first briefly explored a set-up[6] and since then a small number of works on closely related subjects have been carried out, for example[7,8]. More recently, an identical approach has been implemented, but using an electrovalve as flow actuator[9].
An important conclusion of these studies is that the actuator, which is the component that translates the computed flow rate output into a real acoustical flow, has been the main reason for low accuracy.
In the present study, the idea of using a loudspeaker to perform the actuation is investigated. While this transducer is not capable of generating a mean flow, that flow component is known to be unimportant for proper self-sustained functioning[3].
The main development parts of the hybrid instrument are discussed into greater detail in a preceding paper[10].

2 DEVELOPING THE HYBRID INSTSTRUMENT

Figure 2 (a) shows a schematic diagram of a fully functioning hybrid instrument. We will refer to this chart throughout this section and the relevant subsections are also indicated on it.

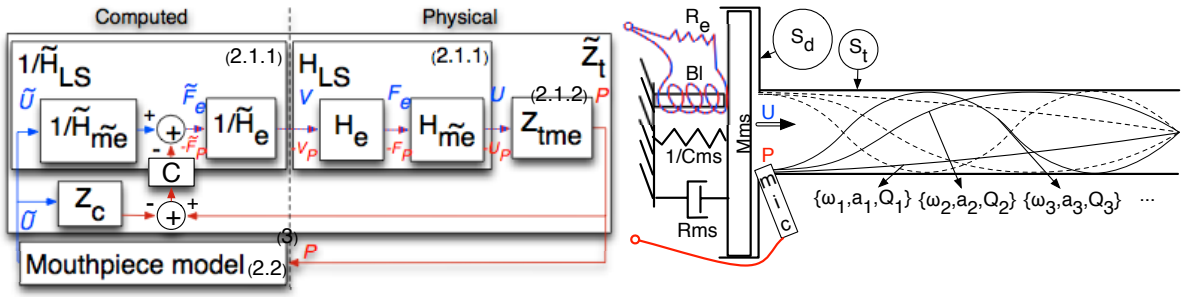

(a) (b)

Figure 2: (a) Flow chart of the hybrid instrument's computed and physical parts. The corresponding sections are indicated between brackets. (b) Outline of the assembled loudspeaker and tube models.

2.1 The Loudspeaker-Resonator System

To begin with, work has been carried out to investigate the behaviour of a loudspeaker mounted on a "clarinet-type" tube: the resonator, as represented in figure 2 (b). We assume that the sound propagates as plane waves, a valid assumption in such small sections for the frequency range of consideration[3]. As the volume between the loudspeaker diaphragm and the tube is small, the change in section size between the loudspeaker (with diaphragm section S_d) and the tube (with section S_t) has negligible influence on both the "volume flow rate" U and the pressure P, so that they can be considered as equal in both places. We will express all equations in the complex s-domain by using the Laplace Transform, with $s = j\omega$ ($\sigma = 0$), $s = j\omega$, $\omega = 2\pi f$ and f the frequency in Hz.

2.1.1 The loudspeaker

Ideally, a flow rate signal calculated by the mouthpiece model should proportionally and directly be converted into a physical flow by the actuator, which means that we need to know the loudspeaker's transfer function.
We adopted a classical small-signal model, initially proposed by Small[11]. It consists of an electrical part with R_e and Bl respectively the DC resistance and coil factor of the voice coil, with input voltage $V(s)$. The mechanical part is modelled by a 1-DOF mass-spring-damper system, and receives a force $F_e(s)$ from the voice-coil. As such, the transfer functions for the electrical (H_e) and mechanical ($H_{\sim me}$) loudspeaker parts are expressed by the ratios of outgoing over incoming signals:

$$H_{\sim me} = \frac{U(s)}{F_e(s)} = \frac{S_d s}{Mms(\omega_s^2 + \frac{\omega_s\, s}{Qts} + s^2)} \quad \text{and} \quad H_e = \frac{F_e(s)}{V(s)} = \frac{Bl}{R_e}, \qquad (1)$$

with Mms, the mass of the moving parts of the loudspeaker, $\omega_s = 1/\sqrt{Mms \cdot Cms}$, the speaker's resonant frequency, Qts the total quality factor, U, the outputted volume flow rate and S_d, the diaphragm surface area. The complete loudspeaker system can then be represented by an overall transfer function that expresses the volume flow rate per input voltage:

$$H_{LS} = \frac{U(s)}{V(s)} = H_e \; H_{\sim me}. \qquad (2)$$

We used a traditional method[11] and a method proposed by Klippel[12] to carry out measurements on a 1" Tang Band loudspeaker of type W1-1070SE. Then, a number of regressions on the measured curves were used to obtain the loudspeaker parameters. Here we only mention the resonance frequency, found at $\omega_s = 2\pi \cdot 63.7 \text{ rad Hz}$ and the mass, estimated at $Mms = 9.11 \cdot 10^{-3} \text{ kg}$. We note that the loudspeaker response contained a phase lag that cannot be taken into account by our model. It progressively lowers the phase, attaining an additional shift of about -20^o at 1 kHz.

For coherent functioning of the hybrid instrument, the calculated flow rate signal by the mouthpiece model $\tilde{U}$ should be acoustically reproduced by the loudspeaker into U. Therefore, a feedforward filter is required to undo the loudspeaker response, which would simply be the inverse of the loudspeaker transfer function (2). The problem is that the loudspeaker response can easily vary close to its resonance frequency. Moreover, other parts in the hybrid system impose slight amplitude and phase deviations, which would have a worse impact around this resonance frequency. Therefore, a loudspeaker is chosen that has a resonant frequency far enough below the playing frequencies. Hence, only the Mms term is of importance and the approximated inverse transfer function can be written as:

$$\tilde{H}_{LS}^{-1} = \tilde{H}_{\widetilde{me}}^{-1} \; \tilde{H}_e^{-1}, \qquad (3)$$

with:

$$\tilde{H}_{\widetilde{me}}^{-1} = \frac{\tilde{F}_e(z)}{\tilde{U}(z)} = \frac{Mms \; (z-1)}{S_d \; T_s \; z} \approx \frac{Mms \; s}{S_d} \text{ and } \tilde{H}_e^{-1} = \frac{V(z)}{\tilde{F}_e(z)} = \frac{R_e}{Bl}. \qquad (4)$$

where the continuous derivative s is approximated by a half-sample delayed (for a causal approximation) discrete approximation (with z the discrete equivalent of s and T_s, the sample time) that can be executed by the real-time computer. An extraneous advantage of the exclusion of the remaining terms is that it results in the removal of the mean flow component out of the signal sent to the loudspeaker.

A second problem occurs when the loudspeaker is mounted on the tube: the pressure waves in front of the membrane become substantial, which evokes a coupled interaction between the loudspeaker and the tube. This issue is accounted for with a feedback filter, following a simple principle based on Newton's third law: in order to undo the force on the loudspeaker diaphragm due to the pressure in front of it, $S_d \; P$, it is necessary to add its inverse to F_e. As P is directly measured by the microphone and F_e can be accessed by using $\tilde{H}_e^{-1}$, the feedback controller is simply:

$$C = -S_d \qquad (5)$$

However, it should be noted that the small (intentional) mouthpiece pressure increase due to the injected flow U has to be left out of this control loop, which is done by subtracting $U \cdot Z_c$ from the measured mouthpiece pressure. The complete system is represented in the flow chart in figure 2.

As for the real-time computer, a recompilation of a Linux kernel on standard PC architecture is used, which is covered by the *Xenomai* framework[13]. For that, we relied on the work by Benacchio et al., who created a patch that inserts the NI acquisition card driver-code into C-code generated by Simulink[14]. As such, a system with a discrete solver and a sampling rate of $f_s = 40 \text{ kHz}$ could be obtained, which is sufficient for our purpose.

2.1.2 The resonator

The resonator employed in our hybrid instrument is a tube whose dimensions roughly match those of a soprano clarinet playing its lowest note. The inner diameter measures 14.2 mm and its length is 58 cm. To be able to compare the hybrid sounds with "entirely simulated" sounds (i.e. where the resonator is also simulated), we use a resonator model based on a modal decomposition of the input impedance that describes each impedance peak as a second order transfer function with real coefficients[15]:

$$Z_t(s) = Z_c \sum_{n=1}^{N} \frac{a_n s}{\omega_n^2 + \frac{\omega_n}{Q_n} s + s^2}, \qquad (6)$$

where $\{a_n, \omega_n, Q_n\}$ are the real modal coefficients: the amplitude, resonance frequency and quality factor of mode n, and $Z_c = \rho c / S_t$ is the characteristic impedance of the resonator, with ρ the density of air, c the speed of sound and S_t the cross-sectional area of the tube. This technique allows approximation of a finite number of modes of the measured impedance with good precision. The modal coefficients are found using an iterative least square fitting method, using eq. (6), on a complex impedance curve measured with the "capillary tube method"[16]. Figure 3 shows the modal approximated impedance curve around the resonant frequencies (in solid green). This curve is found from the measured curve (not plotted) with a ± 2 cent precision for the resonance frequencies and a ± 0.3 dB precision in a large range around the resonances.

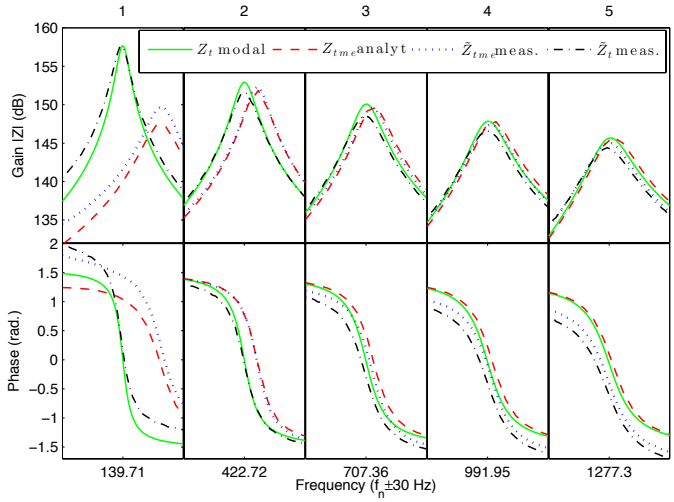

Figure 3: Modal, analytic coupled, measured coupled and measured uncoupled tube impedance curves ± 30 Hz around the five first modes.

We found the calculation of a loudspeaker-coupled tube impedance deviates from the standalone tube impedance the more a defined "coupling frequency": $\omega_{cn} = \sqrt{Z_c S_d^2 a_n / Mms}$ approaches the modal frequencies. The resulting calculated and measured coupled tube impedances for our loudspeaker and tube are presented in figure 3 (in dashed red and dotted blue respectively). Finally, using the filters to account for the loudspeaker, the "restored" impedance curve $\tilde{Z}_t$ is also plotted (in black dash-dotted) in figure 3. The higher modes show phase deviations that are likely due to the mentioned parasitic phase lag, but the result is fairly close to the original measured and modally approximated tube impedance Z_t .

2.2 Single-Reed Mouthpiece Model

As the tube impedance $\tilde{Z}_t$ is the ratio of pressure P and flow rate $\tilde{U}$, both accessible by the computer, it is possible to supply any excitation to allow hybrid self-sustained sounds. In this first investigation, we chose a well-established single-reed mouthpiece model as the exciter.
A low-pass filter was added after the microphone input with a cut-off at 6 kHz, to prevent erroneous feedback (possibly due to the plane-wave approximation becoming invalid).

For the mouthpiece, the classical quasi-static (i.e. the reed dynamics are neglected) model depicted in figure 4 was adopted[1,9].

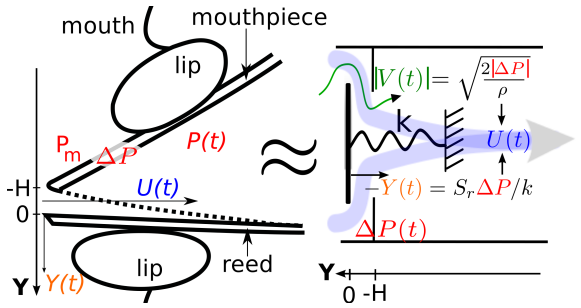

Figure 4: The mouthpiece outline and its quasi-static model.

The air flow that enters the instrument can be expressed as the product of the flow velocity v_f and the effective reed opening section S_f. The former can be found by the Bernoulli theorem applied between the mouth and the reed flow channel (thus between the mentioned pressure difference) and the latter is assumed to be linearly related to the reed displacement[3] Y, which is created by the pressure difference between mouth and mouthpiece interior ($P_m - P$), acting on part of the reed (with stiffness k_r) surface S_r. All together, the volume flow rate and reed displacement are expressed as:

$$U = \underbrace{sign(P_m - P)\sqrt{\frac{2\,|P_m - P|}{\rho}}}_{v_f} \underbrace{\mathcal{H}(Y + H)(Y + H)w}_{S_f} \quad \text{and} \quad Y = \frac{-S_r(P_m - P)}{k_r}. \qquad (7)$$

where ρ is the air density and w is the effective reed width. The $sign$ operator is introduced to make the calculation of negative flows possible and the Heaviside function $\mathcal{H}$ to hold a zero flow rate when the reed hits the lay, which occurs above the "beating pressure" P_M.
This equation can be simplified and normalized (or "nondimensionalized") by defining $p = P / P_M$ and $u = U \cdot P_M / Z_c$:

$$u = sign(\gamma - p)\sqrt{|\gamma - p|}\mathcal{H}(p - \gamma + 1)(p - \gamma + 1), \qquad (8)$$

where ζ lumps all mouthpiece parameters together and $\gamma = P_m / P_M$ represents the normalized mouth pressure.
There are three remaining independent parameters: P_M, which determines the signal amplitude (without timbre variation for a resonator with a linear response in amplitude), the mouth pressure γ and the mouthpiece parameter ζ, which both have an effect on the signal shape and attack, and thus the timbre of the sound[17]. We note that the "oscillation threshold" is the minimum mouth pressure value to obtain a self-sustained state, and lies always above $\gamma = 1/3$ and the dynamic "oscillation extinction" is defined as the γ value where the sound disappears after a continuously increasing mouth pressure.

3 EVALUATION: HYBRID VERSUS SIMULATED INSTRUMENTS

We evaluated the hybrid self-sustained operation by combining the previously described loudspeaker-resonator system with the filters to account for the loudspeaker and with the computed mouthpiece model. The hybrid results are compared with a simulation of the entire instrument, which includes a tube simulation where the loudspeaker is assumed to be a rigid piston with an ideal response.

An important objective is to create an instrument that produces persistent sounds for a listener. Therefore, we calculate a signal related to the pressure waves radiated by the instrument. A simplified yet sufficiently relevant "monopole" radiation model concerns the temporal derivative of the pressure waves propagating downstream from the resonator. It can be verified that this downstream (normalized) pressure corresponds to $(p + u)/2$, so that the approximated external pressure can be written as:

$$p_{ext} = \alpha \frac{d(p+u)}{dt}, \quad (9)$$

where α remains constant over frequency and for a fixed distance from the resonator output.
In order to cope with the amplification of high frequency noises, prior to the derivative a steep (IIR, 33rd order Butterworth) low-pass filter is applied, with its cut-off frequency at $4\ \mathrm{kHz}$, above the resonance frequency of the upper simulated mode.

To allow for a quantitative and relevant comparison of hybrid and simulated sounds, we use so called "sound descriptors". These represent a standardized set of features that describe relational values derived from the spectral, temporal and harmonic representations of the sound. Sound descriptors can be meaningful characteristic features regarding both perception (to quantize the timbre mostly) and the instrument's acoustic functioning.
For the selection of useful descriptors, we rely on the work of Barthet, who extensively studied the clarinet timbre and it's relation to the instrument's input parameters[18,19]. His work resulted in the abstraction of a clarinet-related three-dimensional perceptive timbre space, based on the classification of a set of clarinet-synthesized sounds (using a realistic temporal mouth pressure envelope) by listeners. Then, an algorithmic procedure allowed us to relate the descriptors of the concerning sounds to these dimensions, allowing for the correlation between the dimensions and the sound descriptors. For our study, we chose to adopt a number of highly correlated descriptors that are also of perceptive relevance: the "Logarithmic Attack Time" (LAT), the "Spectral Centroid" (SC), and the "Odd/Even harmonics Ratio" (OER). The LAT descriptor represents the logarithm (at a decimal base) of the time comprised between the moments the amplitude envelope reaches 10% and 80% of the maximum amplitude value of the sound event. The SC represents the frequency of the centre of the spectrum, using the amplitude weight of each frequency, and has a robust connection with the perceptive impression of "brightness" of a sound. The OER is calculated as the ratio of odd and even harmonic amplitude components. While the cylindrical closed-open resonator stimulates an odd frequency spectrum, the mouthpiece model can also introduce even frequency components, which motivates the examination of this descriptor.
In addition, we studied the fundamental frequency (f_0) and the mean (RMS) pressure evolution. Given the known typical progression of the RMS mouthpiece pressure as a function of the mouth pressure progression[20], we calculated the RMS of p rather than p_{ext}. Furthermore, we also report the end of the attack time (EAT), which is the time when the amplitude envelope reaches 80% of its maximum, relative to the start of blowing. In contrast to the LAT, this time span expresses the delay between the mouth pressure onset and the resulting sound onset, which is an important aspect regarding the timing of played notes.
For the precise mathematical definition of all these descriptors we refer to Barthet[18] and Peeters[21]. The calculation of the descriptors is carried out with the MATIMBRE toolbox, a MATLAB® program developed by Barthet[18,19].

In a first part, continuous mouth pressure γ progressions for several embouchure parameter ζ values are studied to observe sound features comprised in the spectrum of the sustained sound, using the mentioned spectral descriptors. Then, the attack times of individual sounds for several γ and ζ values are investigated with the LAT and EAT descriptors. All measurements are performed with a beating pressure of $P_M = 100\ \mathrm{Pa}$.

3.1 Sustained Sounds

Since the resonator simulation is limited to 14 modes, we only took into account that part of the spectrum, i.e. up to $3900\ \mathrm{Hz}$. The OER descriptor relies on a number of harmonic peaks in the spectrum, which we set to 20 (both odd and even) harmonics, as above sometimes wrong peaks were identified.
We varied the normalized mouth pressure γ from 0.33 to 2.1 for six values of ζ (between 0.1 and 0.35). Figure 5 (a) shows the temporal pressure waves produced by the hybrid and simulated

instruments for two arbitrary input parameter states: $\{\zeta = 0.15, \gamma = 0.8\}$ and $\{\zeta = 0.35, \gamma = 1.7\}$. It can be seen that the amplitudes and wavelengths are closely matching and that the wave shapes also reasonably correspond. Figure 5 (b) shows the spectra corresponding to the first mentioned state. The first four odd harmonics match very well, then the higher harmonics from the simulation decrease slightly faster then the hybrid harmonics, which is globally observed for all sounds resulting from the mentioned input parameter range. Given that higher frequencies are increasingly important in the external pressure, it can be expected that the harmonics amplitude deviation will have its consequences on the spectrum-based descriptors.

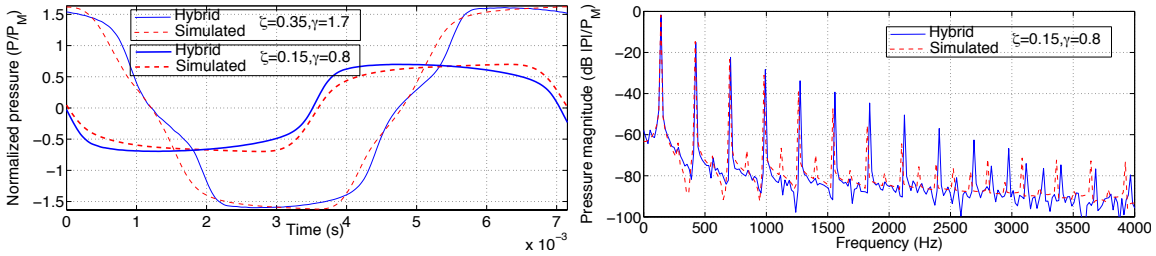

(a) (b)

Figure 5: Pressure signals in the hybrid (plain blue) and simulated (dashed red) mouthpieces. (a) represents temporal signals for two $\{\zeta, \gamma\}$ input parameter states, and (b) shows the spectra of one state.

The mentioned descriptors evolutions are represented in figure 6. The hybrid and simulated RMS evolutions and extinctions in part (a) are properly corresponding and also match to findings in the literature[20], while the hybrid note onsets appear slightly before the simulated onsets. It should be mentioned that for $\zeta = 0.1$, a parasitic low frequency pressure burst has disturbed the hybrid measurement, which explains the deviation between hybrid and simulated note onsets and extinction times.

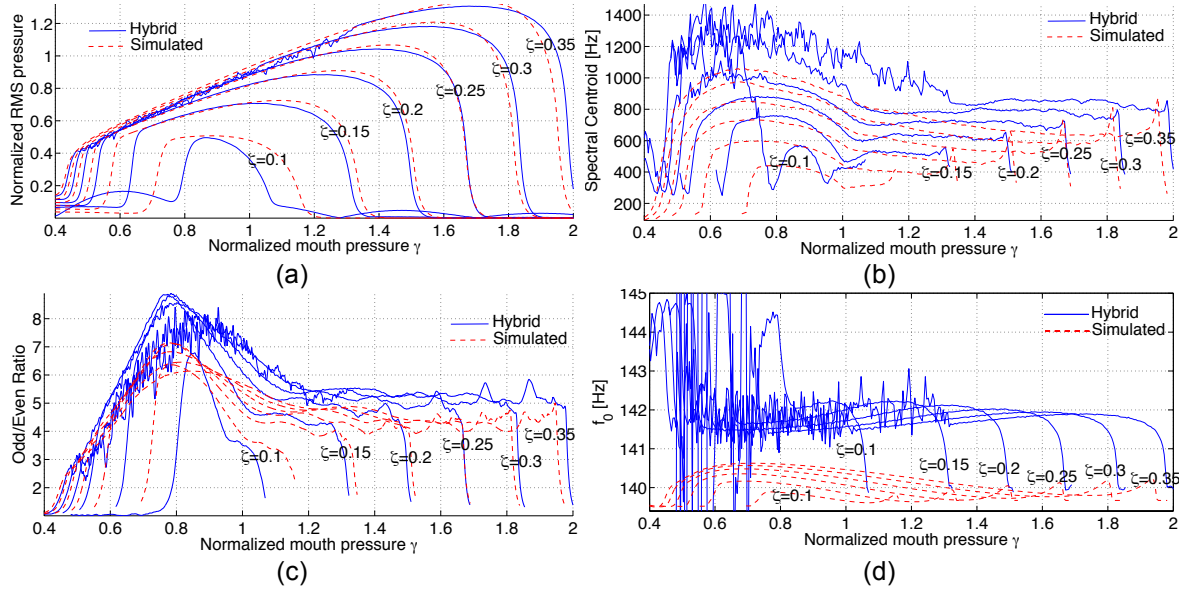

(a) (b) (c) (d)

Figure 6: Sound descriptors for sustained sounds, produced with a hybrid (solid blue) and simulated (dashed red) instrument for six ζ values and an increasing γ. (a) the RMS envelopes of the mouthpiece pressure. (b) the Spectral Centroids, (c) the Odd/Even Ratios and (d) the fundamental frequencies of the calculated external pressure.

For $\zeta \geq 0.3$ and in a range that starts from low γ values, a hybrid unstable state is encountered, introducing a parasitic high-pitched creaking. Closer signal observations indicate that this occurs

when the reed is in fully opened position during self-sustained operation, where a steep flow-rate variation applies for small pressure variations. Moreover, an observation of the flow rate signal revealed that this also slightly occurs for the simulated instrument when $\zeta \geq 0.35$, which possibly demands a revision of the used physical mouthpiece model (given that this effect doesn't occur in real reed instruments). Furthermore, it is very likely that the superior hybrid instability is related to the derivative in $\tilde{H}_{LS}^{-1}$.
The Spectral Centroids in part (b) confirm the earlier made assumption concerning the slightly increased hybrid higher harmonics, which explains why the hybrid SC's are superior to the simulated ones. Nevertheless, their progressions are similarly increasing up to $\gamma = 0.7$, to then decrease until the note extinction.
The Odd/Even Ratio curves in part (c) explain that the simulation globally produces relatively more even harmonics than the simulation does. Both curves follow a similarly shaped evolution, with a maximum peak around $\gamma = 0.8$ (maxima for $\zeta = 0.15$ to $\zeta = 0.25$), and rapidly decreasing before and after that mouth pressure.
The fundamental frequency evolutions represented in part (d) show a far less corresponding result between hybrid and simulated sounds. While the simulation starts of at a fundamental frequency close to the first modal frequency of $139{,}7\ \mathrm{Hz}$, and then slightly deviates with a progression comparable to the Spectral Centroid, the hybrid sound starts a few Hz above that frequency (we note that the temperature consistency is considered) and follows a mostly opposite progression to rapidly decrease to the first modal frequency when the extinction is approached. A possible reason for this aberrant phenomenon might be the shifted phase response of the first mode of $\tilde{Z}_t$, which indeed would stimulate a slight frequency increase. Another (or coinciding) explanation is that the upper modes follow a positively increasing inharmonicity, which could indicate that the hybrid self-sustained operation is likely more maintained by these modes.

We found very closely matching hybrid results (for the simulation these curves are invariant) for P_M from $12\ \mathrm{Pa}$ to $400\ \mathrm{Pa}$. Below that range, the noise becomes substantial and above, loud and spectrally rich sounds start to saturate. It should be noted that these values lie far below the realistic beating pressures, which lie in between $P_M = 4\ \mathrm{kPa}$ and $P_M = 10\ \mathrm{kPa}$. Therefore, this hybrid instrument can only be used for cases where the assumption of resonator amplitude linearity is valid. Moreover, additional measurements with $P_M = 100\ \mathrm{Pa}$ proved precise hybrid repeatability. However, there is an unknown factor that can considerably alter the extinction thresholds and, to a smaller degree, the oscillation thresholds, so that further investigation is required.

3.2 Attack Transients

Using the same ζ values, ten constant γ_m values between 0.4 and 1.2 were evaluated. For a realistic situation, the mouth pressure is gradually introduced. Since for certain ζ values, the attack time is very short, an even quicker γ increase is required, not to influence the attack time, so that we opted for a rise time of $0.3\ \mathrm{s}$ to reach γ_m from 0. However, given that γ values close to 0 evoke an unstable state, it is ascertained that γ never goes below 0.3 during the hybrid performance, which doesn't affect the sound as that value still lies under the oscillation threshold.
Figure 7 shows the resulting Logarithmic Attack Times in part (a) and the End of the Attack Times in part (b), for both hybrid and simulated instruments.

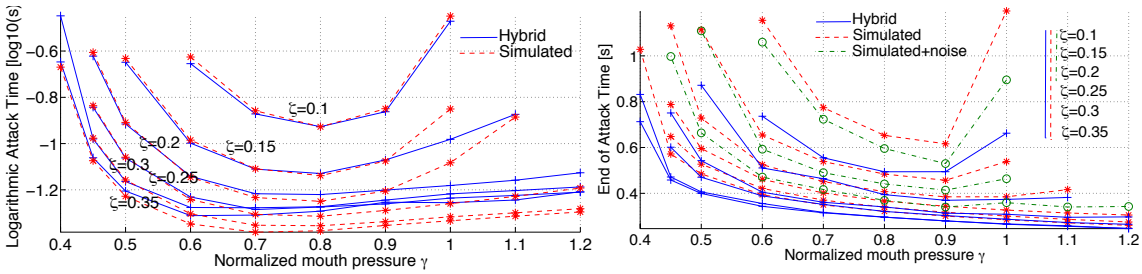

(a) (b)

Figure 7: Sound descriptors for the attack sounds produced with the hybrid (solid blue) and simulated (dashed red) instruments for six ζ values and ten γ values. (a) shows the logarithmic attack times and (b) the end of the attack times. (b) also includes a simulation with added noise (dot-dashed green) for the lowest three ζ values.

While the hybrid and simulated LAT results in a very good correlation for a large range of input parameters, the actual sound onsets, indicated by the EAT, shows important deviations, in particular for low ζ values. We suppose that the supplementary delay in the simulations may be due to the absence of irregularities that may stimulate the attack, such as noises (which are also present in real wind instruments, due to the flow turbulence). Therefore, we carried out another simulation with an added noise signal to the mouthpiece pressure (with a normalized amplitude of 0.008, corresponding to the observed hybrid noise level.) The result is added to the EAT graph (in green dash-dotted) for the first three ζ values. This experiment revealed that the EAT reduced up to 30% compared to the noiseless simulations, which partly confirms our assumption. Given the importance of timing, this aspect might be of consideration for reed instrument physical models. We note that the added noise did not significantly influence the LAT.
Also, on repeating the experiments several times, the results were closely verified and corresponding conclusions for the mentioned P_M range were found.

4 CONCLUSIONS AND PERSPECTIVES

The development of a hybrid wind instrument, by means of a loudspeaker has been successfully implemented in theory and practice.
In the first instance, the development of the instrument is described. The loudspeaker is studied and a feedforward and feedback filter is proposed to account for its response when mounted on the resonator. A resonator model is proposed and its impedance curves are compared to curves obtained with the mounted loudspeaker, which demonstrated the effectiveness of the filters. Then, a typical quasi-static mouthpiece model is explained.
In a next stage, the hybrid instrument is evaluated by comparing the sounds (with appropriate descriptors) to an entirely simulated version. Firstly, six values for the embouchure parameter ζ are tested for continuously increasing mouth pressure values γ to observe the sustained sound, and then for ten constant γ values for a study of the attack times.
The overall hybrid and simulated descriptors are reasonably close, particularly for the shape of their progression. Only the slight fundamental frequency variations appeared to be contradicting. While a very good attack time resemblance is found, the actual attack onsets could differ. Further, a coherent dynamic range for $P_M = 12$ Pa to 400 Pa and good repeatability has been found.
All together, it can be said that these results attest for a fairly coherent performance of the hybrid instrument, which shows the suitability of using a loudspeaker as the actuator for hybrid wind instrumentation that can serve to answer questions in both acoustical wind research and in musical research contexts.
Nevertheless, several features are difficult to explain due to the phenomenological character of this investigation. Therefore, a further work will involve an input flow rate measurement performed during hybrid operation, which will allow for a better identification of the remaining failures.

5 ACKNOWLEDGMENTS

This work is supported by the Open University, Milton Keynes. Special thanks goes to Simon Benacchio and his team at IRCAM, who devoted their time, effort and space to help me copying their real-time computer set-up, and to Mathieu Barthet, who provided me with his MATIMBRE toolbox for the sound descriptor calculations.

6 REFERENCES

1. Wilson TA, Beavers GS. Operating modes of the clarinet. *J Acoust Soc Am*. 1974;56:653-658.
2. Ferrand D, Vergez C. Blowing machine for wind musical instrument : toward a real-time control of the blowing pressure. *2008 16th Mediterr Conf Control Autom*. 2008.
3. Hirschberg A. Aero-acoustics of wind instruments. In: A. Hirschberg J. Kergomard, Weinreich G, eds. *Mechanics of Musical Instruments*. Wien: Springer; 1995.
4. Boulez P. Timbre and composition - timbre and language. *Contemp Music Rev*. 1987;2, part. 1:169.
5. Farwell N. Being what I Am: Doing what I Do; Manifesto of a Composer. 2001.
6. Maganza C. Excitations non linéaire d'un conduit acoustique cylindrique. Observations de doublements de période précédant un comportant chaotique. Application à la Clarinette. 1985.
7. Guérard J. Modélisation numérique et simulation expérimentale de systèmes acoustiques - Application aux instruments de musique. 1998.
8. Grand N. Etude du seuil d'oscillation des systèmes acoustiques non-linéaires de type instrument à vent. 1994.
9. Buys K, Vergez C. A hybrid reed instrument: an acoustical resonator with a numerically simulated mouthpiece. In: *Proceedings of Acoustics 2012*. Nantes; 2012.
10. Buys K, Sharp D, Laney R. Developing a hybrid wind instrument : using a loudspeaker to couple a theoretical exciter to a real resonator. In: *Proceedings of the International Symposium on Musical Acoustics*.; 2014.
11. Small RH. Direct Radiator Loudspeaker System Analysis. *J Audio Eng Soc*. 1972;20(5):383-395.
12. Klippel W, Seidel U. Fast and accurate measurement of linear transducer parameters. *Prepr Eng Soc*. 2001:1-7.
13. Xenomai: Real-Time Framework for Linux. Available at: http://www.xenomai.org/. Accessed May 6, 2014.
14. Benacchio S, Piéchaud R, Mamou-Mani A. Active Control of String Instruments using Xenomai. In: *15th Real Time Linux Workshop*.; 2013.
15. Silva F, Kergomard J, Vergez C, Gilbert J. Interaction of reed and acoustic resonator in clarinetlike systems. *J Acoust Soc Am*. 2008;124(5):3284-3295. doi:http://dx.doi.org/10.1121/1.2988280.
16. Sharp DB, Mamou-Mani a., van Walstijn M. A Single Microphone Capillary-Based System for Measuring the Complex Input Impedance of Musical Wind Instruments. *Acta Acust united with Acust*. 2011;97(5):819-829. doi:10.3813/AAA.918462.
17. Chaigne A, Kergomard J. *Acoustique des instruments de musique*. Belin; 2008.
18. Barthet M, Guillemain P, Kronland-Martinet R, Ystad S. From Clarinet Control to Timbre Perception. *Acta Acust united with Acust*. 2010;96(4):678-689. doi:10.3813/AAA.918322.
19. Barthet M. De l'interprète à l'auditeur : une analyse acoustique et perceptive du timbre musical. 2009;(Ed 353).
20. Atig M, Dalmont J-P, Gilbert J. Saturation mechanism in clarinet-like instruments, the effect of the localised non-linear losses. *Appl Acoust*. 2004;65(12):1133-1154. doi:10.1016/j.apacoust.2004.04.005.
21. Peeters G, Giordano BL, Susini P, Misdariis N, McAdams S. The Timbre Toolbox: Extracting audio descriptors from musical signals. *J Acoust Soc Amer*. 2011;130(5):2902-2916. doi:10.1121/1.3642604.